

Thermal expansion in zircon and almandine: Synchrotron x-ray diffraction and lattice dynamical study

S. L. Chaplot,¹ R. Mittal,¹ E. Busetto,² and A. Lausi²

¹*Solid State Physics Division, Bhabha Atomic Research Centre, Trombay, Mumbai 400 085, India*

²*Sincrotrone Trieste, SS 14, Km 163.5, 34012 Basovizza, Trieste, Italy*

(Received 6 March 2002; published 12 August 2002)

X-ray diffraction data are obtained on polycrystalline samples of zircon (ZrSiO_4) and almandine ($\text{Fe}_3\text{Al}_2\text{Si}_3\text{O}_{12}$) from 100 to 300 K using x-ray diffraction beam line at Elettra synchrotron source. The observed thermal expansions in zircon and almandine, which differ by a factor of 2–3, are found to be in good agreement with the predictions from our lattice-dynamical calculations. The calculations also enabled a microscopic interpretation of the available experimental data.

DOI: 10.1103/PhysRevB.66.064302

PACS number(s): 63.20.Dj, 65.40.De, 61.10.Nz

I. INTRODUCTION

In a comprehensive study of the structure, dynamics, and thermodynamics of important materials, the thermal expansion behavior forms an important component since it allows one to probe the anharmonicity of an interatomic interaction potential. In this context, low-temperature data are of special interest where quantum-mechanical aspects of dynamics are particularly important. The subject of thermal expansion has received a boost due to the discovery of an unusually large negative thermal expansion in ZrW_2O_8 .¹ Earlier using a combination² of lattice dynamics and high-pressure inelastic neutron-scattering experiments we have successfully explained the negative thermal expansion behavior in ZrW_2O_8 . In this paper we report our experimental and theoretical study of thermal expansion in two important materials, namely, zircon ZrSiO_4 and almandine $\text{Fe}_3\text{Al}_2\text{Si}_3\text{O}_{12}$, which have polyhedral structural units but show a normal thermal-expansion behavior. The thermal expansion in the two materials differs by a factor of 2–3.

Zircon ZrSiO_4 (body-centered-tetragonal cell, space group $I4_1/amd$) is an important host silicate mineral for heat producing radioactive elements uranium and thorium in the earth's crust. The mineral is found in igneous rocks and sediments. Several workers have reported a zircon to scheelite structure phase transition³ in static high pressure and shock experiments. ZrSiO_4 scheelite is one of the most incompressible compounds⁴ containing SiO_4 tetrahedra. A high-temperature neutron-powder-diffraction study⁵ of zircon carried out up to 1900 K showed a displacive phase transition at 1100 K, and further decomposition in ZrO_2 and SiO_2 at 1750 K.

Garnets have several important applications in computer memories, lasers, microwave optical elements, etc. Silicate garnets have been used^{6–8} in geothermometers and geobarometers for crustal and mantle rocks. Extensive studies^{9–14} have been reported on garnet almandine $\text{Fe}_3\text{Al}_2\text{Si}_3\text{O}_{12}$ (body-centered-cubic cell, space group $Ia\bar{3}d$) on crystal structure, lattice vibrations, thermal expansion, etc.

We earlier reported inelastic neutron-scattering experiments and detailed lattice-dynamical calculations of zircon¹⁵

and almandine.¹⁴ The experimental data of the variation of unit-cell volume with temperature for zircon⁵ and almandine^{12,13} have been available above room temperature while the structure^{9,10} of almandine at 100 K is also known. We have now obtained the structural variation between 100 and 300 K in both zircon and almandine from x-ray diffraction measurements, using 5.2 R beam line at Elettra synchrotron radiation source. We have also analyzed the thermal expansion in these compounds using the lattice-dynamical shell model. The organization of the paper is as follows: Sec. II gives the experimental details while Sec. III describes the lattice-dynamical studies. A discussion of the results is given in Sec. IV while Sec. V presents the conclusions.

II. EXPERIMENT

We have obtained x-ray diffraction data using the 5.2 R x-ray diffraction beam line at the Elettra synchrotron source. We used polycrystalline natural samples of zircon and almandine. The x-ray diffraction powder profiles were obtained at several temperatures in the range of 100–300 K in steps of 10 or 20 K. A cryostream was used for keeping the samples at different controlled temperatures. The temperature stability was 0.5 K from 100 to 220 K. Above 220 K the stability was 4 K. The samples were kept inside a glass capillary of 1 mm inner diameter and rocked during the measurements to reduce the systematic errors due to preferred orientations and inadequate powder averaging. The beam size was chosen to be 0.1 mm. An image plate was used for recording the data. The image plate was of 345 mm diameter and having 2300 pixels diametrically. The diffraction data were recorded with a wavelength (λ) of 1 Å and bandwidth ($\Delta\lambda/\lambda$) of 10^{-3} . The sample to the image plate distance (112.38 mm) and wavelength (0.9992 Å) of the incident x-ray beam was calibrated using data taken on a silicon sample at 300 K with the program FIT2D.¹⁶ In this configuration, we could measure the diffraction data upto $\sin(\theta)/\lambda$ of about 0.5.

III. LATTICE-DYNAMICAL CALCULATIONS

Lattice dynamics calculations of the vibrational and thermodynamic properties can be carried out using either a

quantum-mechanical *ab initio* approach or using semiempirical interatomic potentials. *Ab initio* calculations of phonon modes at the Brillouin zone center have been reported for zircon.¹⁷ In view of the structural complexity of these compounds, the present calculations, involving integration over the whole Brillouin zone and volume dependence of phonon modes, have been carried out using semiempirical interatomic potentials.

We have now used the same interatomic potential model as in our previous studies of zircon and almandine.^{14,15} The interatomic potentials consist of Coulombic and the short-ranged Born-Mayer-type interaction terms, van der Waals interactions, and Si-O bond-stretching potential.^{14,15} The polarizability of the oxygen atoms is introduced in the framework of the shell model.^{14,15,18} The empirical parameters are optimized to reproduce the minimum enthalpy structure close to that determined by the diffraction experiments at zero pressure. Further the potential parameters are chosen such that they satisfy the condition of dynamic equilibrium, and long-wave-length phonon modes and elastic constants are close to their experimental values. The potential reproduces the structure of zircon and almandine quite satisfactorily. The phonon frequencies as a function of wave vectors in the entire Brillouin zone and its volume dependence are calculated using a program¹⁹ developed by us. The calculations are carried out in the quasiharmonic approximation. In this approximation

the crystal structure at each pressure is obtained by minimization of the free energy.¹⁸

In quasiharmonic approximation the volume thermal expansion coefficient is given by

$$\alpha_V = \frac{1}{BV} \sum_i \Gamma_i C_{Vi}(T), \quad (1)$$

where V is the unit cell volume, B is the bulk modulus, Γ_i ($= -\partial \ln E_i / \partial \ln V$) and C_{Vi} are the mode Grüneisen parameter and specific-heat contributions, respectively, of the phonons in state i ($= \mathbf{qj}$).

The volume thermal expansion in zircon and almandine is determined by integrating over the contribution of phonons of 512 and 28 wave vectors, respectively, in the irreducible Brillouin zone. In view of the large lattice spacing (around 11.5 Å) of almandine, its Brillouin zone is quite small. The dispersion is therefore small and the contribution of phonons

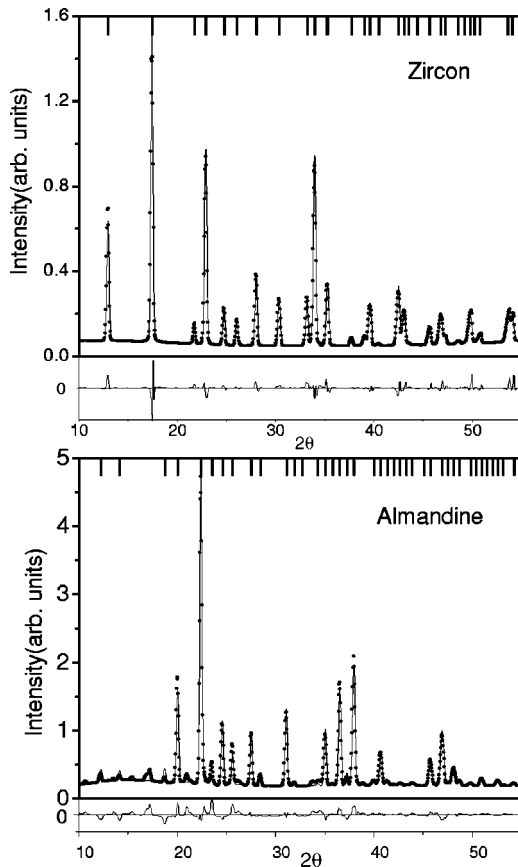


FIG. 1. The Reitveld refinement of powder-diffraction patterns of zircon (ZrSiO_4) and almandine ($\text{Fe}_3\text{Al}_2\text{Si}_3\text{O}_{12}$) at 100 K.

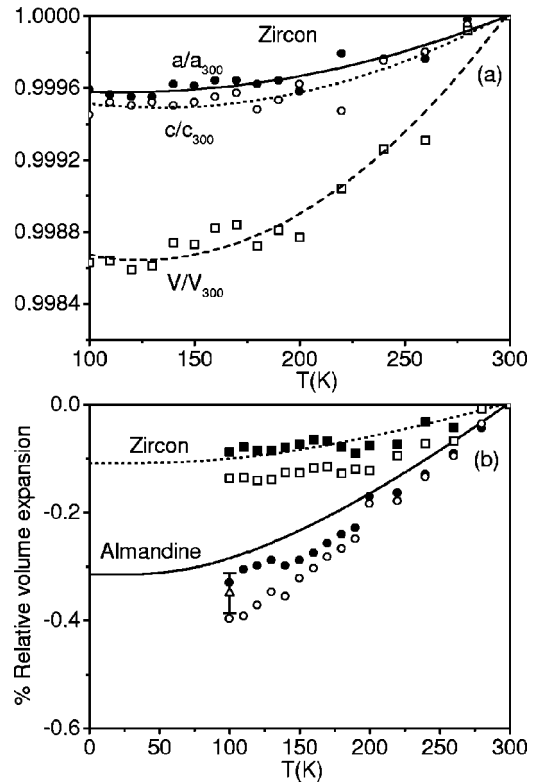


FIG. 2. (a) The experimental data on variation of cell parameters and unit-cell volume with temperature for zircon from the second data set (see text). The lines through the data are guides to the eye. (b) The comparison of the calculated and experimental data of unit-cell volume with temperature from two different data sets for zircon and almandine. The estimated coordinates of the centre-of-image plate for zircon in two data sets are (1151.7,1149.5) and (1150.7,1150.5), respectively, while for almandine the corresponding coordinates are (1150.4,1148.5) and (1150.7,1150.5). The present experimental data from the first and second set are shown using closed and open symbols, respectively. R factors of the Reitveld refinement are nearly the same in the two data sets (see text). The differences of the result from the two data sets reflect their precision. The experimental data for almandine from Ref. 10 at 100 K is shown by a triangle.

TABLE I. The structure parameters of zircon and almandine. In zircon (space group $I4_1/amd$) the atom positions are at Zr(0, 0.75, 0.125), Si(0, 0.25, 0.375) and O(0, u,v). In almandine (space group $Ia\bar{3}d$) the atom positions are at Fe(0, 0.25, 0.125), Al(0, 0, 0), Si(0.375, 0, 0.25), and O(u,v,w). The literature data on zircon and almandine are from Refs. 5 and 10, respectively. The number in parentheses refers to the errors in the last digit as determined by the fitting procedure.

		Data set I		Data set II		Literature	
		100 K	300 K	100 K	300 K	100 K	293 K
Zircon	a (Å)	6.5991(1)	6.6007(1)	6.5963(2)	6.5989(2)	6.610(5)	
	c (Å)	5.9841(1)	5.9866(2)	5.9824(3)	5.9857(3)	6.001(5)	
	u	0.0601(5)	0.0581(5)	0.0598(6)	0.0582(5)	0.0646(4)	
	v	0.1947(5)	0.1945(5)	0.1950(6)	0.1950(5)	0.1967(3)	
Almandine	a (Å)	11.5026(4)	11.5152(4)	11.5004(3)	11.5156(3)	11.512(1)	11.525(1)
	u	0.0355(5)	0.0356(5)	0.0356(4)	0.0362(5)	0.03395(3)	0.03401(3)
	v	0.0472(5)	0.0467(5)	0.0466(5)	0.0456(5)	0.04943(3)	0.04901(4)
	w	0.6560(6)	0.6558(6)	0.6559(5)	0.6556(6)	0.65268(4)	0.65278(4)

of 28 wave vectors in the irreducible Brillouin zone is found to be sufficient for the calculations of almandine. The higher-order contribution^{20,21} to thermal expansion arising from the variation of phonon frequencies and bulk modulus with volume has also been included. These effects are important only at high temperatures.

IV. RESULTS AND DISCUSSION

The two-dimensional data from the image plate are converted into one-dimensional powder-diffraction patterns using the program FIT2D.¹⁶ This program allows one to determine the coordinates of the center-of-image plate through selection of a few points on the circular intense rings of powder-diffraction peaks. We have created two slightly different sets of one-dimensional data for zircon and almandine by selecting the coordinates of the center-of-image plate in two independent attempts. We find that although there are negligible differences in the results of the structure refinement from the two data sets, the differences appear relatively large in the estimated thermal expansion as that required a greater precision. Our results from the two data sets therefore provide a measure of the precision achieved in the estimated thermal expansion.

The experimental data for both the sets for zircon and almandine are analyzed using the Reitveld profile refinement technique using the program DBWS9411.²² The pseudo-Voigt function is used to represent individual peaks. The R factors are nearly same from the refinement of both the sets of data. The R factors from the refinement of zircon data from the first (second) set are $R_p = 4.5(5.1)$ and $R_{wp} = 6.2(7.2)$. However, the diffraction peaks are slightly sharper for the second set of data by about 5–10%. The refined diffraction pattern from the second set of data at 100 K for zircon is shown in Fig. 1. The variation of unit-cell parameters and cell volume from the refinement of second data set are shown in Fig. 2(a). In Fig. 2(b) we have shown the relative volume expansion

from both the data sets from 100–300 K.

The diffraction pattern for almandine from the second data set is also shown in Fig. 1. The R factors for almandine from the first (second) set of data are $R_p = 7.4(7.2)$ and $R_{wp} = 10.5(10.4)$. The x-ray diffraction data of almandine contain two extra peaks at angles below 25° . We have also carried out a two-phase refinement for almandine including

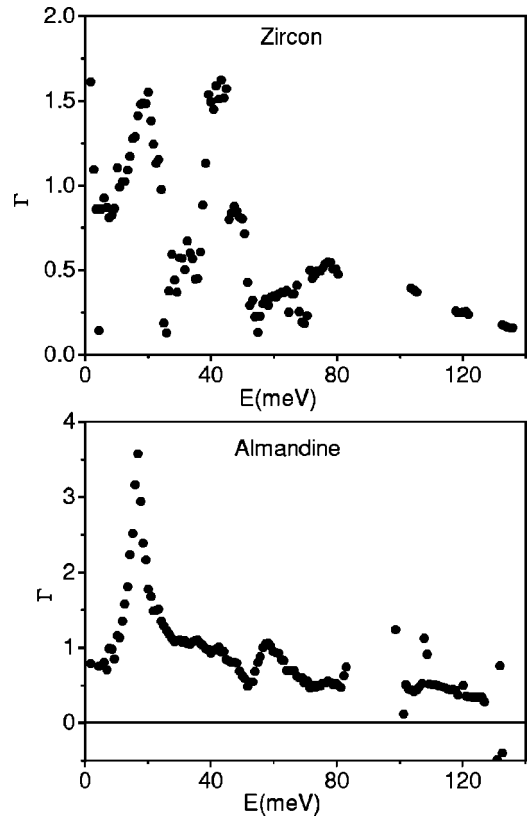


FIG. 3. The calculated mode Grüneisen parameter $\Gamma(E)$ averaged for phonons of energy E for zircon and almandine.

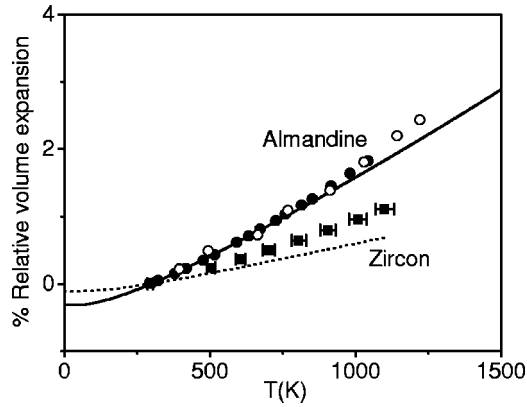


FIG. 4. Comparison between the calculated (dashed line for zircon, full line for almandine) and experimental data (symbols) of cell volumes at different temperatures for zircon (ZrSiO_4) and almandine ($\text{Fe}_3\text{Al}_2\text{Si}_3\text{O}_{12}$), $(V_T/V_{300}-1)\times 100\%$, V_T and V_{300} being the cell volumes at temperatures T and 300 K, respectively. The experimental data for zircon are from Ref. 5 (closed square) and for almandine are from Refs. 12 (closed circle) and 13 (open circle).

quartz SiO_2 as the second phase. The R factors from the two-phase refinement of almandine data (second set) are $R_p = 6.7$ and $R_{wp} = 9.6$. The unit-cell parameters of almandine remain the same with and without the refinement including SiO_2 . The relative volume thermal expansion for almandine for both the sets of data from 100–300 K is shown in Fig. 2(b). The experimental data^{9,10} on the crystal structure for almandine are available at 100 K, which are in agreement with our results [Table I and Fig. 2(b)]. In case of both zircon and almandine the atomic fractional coordinates remain nearly the same at all the temperatures from 100 K to 300 K.

The lattice-dynamical model is used for the calculation (Fig. 3) of the Grüneisen parameter $[\Gamma(E)]$ as a function of phonon energy averaged over the whole Brillouin zone. While $\Gamma(E)$ shows two peaks at 20 meV and 40 meV in zircon, for almandine there is only single peak at about 20 meV. The average value of Γ over the whole Brillouin zone is 0.61 and 1.1 for zircon and almandine, respectively. The calculation of thermal expansion obtained through Eq. (1) is in agreement with our experimental data below 300 K [Fig. 2(b)] and the available data above room temperature (Fig. 4) for zircon and almandine from Ref. 5 and Refs. 12 and 13, respectively. The observed thermal expansion in zircon and almandine, which is different by a factor of 2–3 in the two materials, is found to be in good agreement with the predictions from our lattice-dynamical calculations.

In Fig. 5 we show the contribution of various phonons to the thermal expansion as a function of phonon energy at 100 K, 300 K and 1000 K for both these compounds. In the case of zircon, the maximum contribution to α_V at 100 K is from phonons of energy around 20 and 40 meV, and that at 300 K and 1000 K is largely from around 40 meV energy phonons. In almandine the contribution from around 20 meV phonons is maximum at all the temperatures although progressively higher-energy phonons contribute at higher temperatures. The calculated partial density of states^{14,15} for different atoms shows that at 20 meV the contribution to the phonon

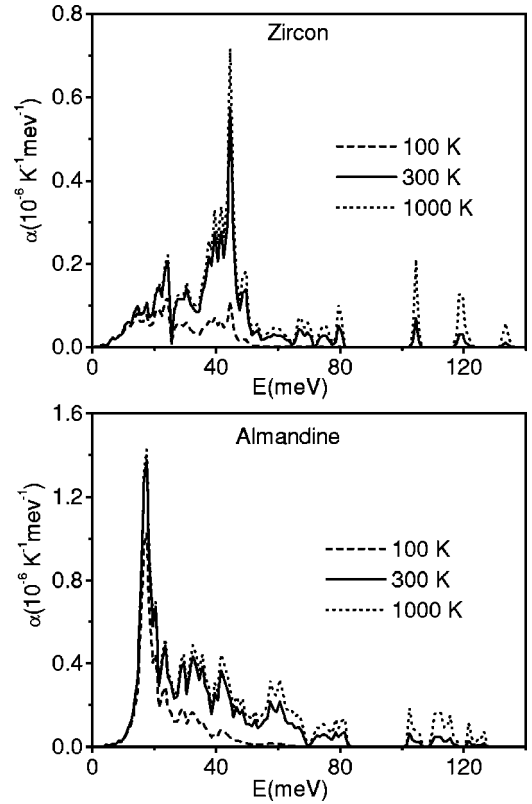


FIG. 5. The contribution of phonons of energy E to the volume thermal expansion as a function of E at 100 K, 300 K, and 1000 K in zircon and almandine.

density of states is mainly due to Zr and Fe atoms in zircon and almandine, respectively. In zircon the contribution at 40 meV is due to all the atoms.

V. CONCLUSIONS

We have reported the x-ray diffraction measurements for zircon and almandine from 100–300 K. The experimental data are used for obtaining the thermal-expansion behavior for both these compounds. The thermal-expansion coefficient is two to three times larger in almandine than in zircon, which is in good agreement with the predictions from our lattice-dynamical calculations. The lattice-dynamical calculations are also helpful in understanding the contribution of various phonons to the total thermal expansion. These studies enabled a microscopic interpretation of the available experimental data and the interatomic potentials have been useful in successfully deriving the thermal-expansion behavior of zircon and almandine.

ACKNOWLEDGMENTS

We thank Dr. A. Savoia and Dr. M. Kopecky for their advice during the experiments. The financial support from DST (India) and MFA (Italy) is also gratefully acknowledged.

- ¹T.A. Mary, J.S.O. Evans, T. Vogt, and A.W. Sleight, *Science* **272**, 90 (1996).
- ²R. Mittal and S.L. Chaplot, *Phys. Rev. B* **60**, 7234 (1999); R. Mittal, S.L. Chaplot, H. Schober, and T.A. Mary, *Phys. Rev. Lett.* **86**, 4692 (2001); S.L. Chaplot and R. Mittal, *ibid.* **86**, 4976 (2001).
- ³E. Knittle and Q. Williams, *Am. Mineral.* **78**, 245 (1993), and references therein.
- ⁴H.P. Scott, Q. Williams, and E. Knittle, *Phys. Rev. Lett.* **88**, 015506 (2002).
- ⁵Z. Mursic, T. Vogt, H. Boysen, and F. Frey, *J. Appl. Crystallogr.* **25**, 519 (1992).
- ⁶N. Funamori, T. Yagi, N. Miyajima, and K. Fujino, *Science* **275**, 513 (1997); T. Kato and M. Kumazawa, *Nature (London)* **316**, 803 (1985).
- ⁷G. Barrow, *J. Geol. Soc. (London)* **49**, 330 (1983).
- ⁸L.Y. Arnovich and R.G. Berman, *Am. Mineral.* **82**, 345 (1997).
- ⁹T. Armbruster, C.A. Geiger and G.A. Lager, *Am. Mineral.* **77**, 512 (1992).
- ¹⁰C.A. Geiger, T. Armbruster, G.A. Lager, K. Jiang, W. Lottermoses, and G. Amthanes, *Phys. Chem. Miner.* **19**, 121 (1992).
- ¹¹A.M. Hofmeister and A. Chopelas, *Phys. Chem. Miner.* **17**, 503 (1991); *Am. Mineral.* **81**, 418 (1996).
- ¹²B.J. Skinner, *Am. Mineral.* **41**, 428 (1956).
- ¹³L. Thiblot, J. Roux, and P. Richet, *Eur. J. Mineral.* **10**, 7 (1998).
- ¹⁴R. Mittal, S.L. Chaplot, N. Choudhury, and C.-K. Loong, *Phys. Rev. B* **61**, 3983 (2000); R. Mittal, S.L. Chaplot, and N. Choudhury, *ibid.* **64**, 094302 (2001).
- ¹⁵R. Mittal, S.L. Chaplot, Mala N. Rao, N. Choudhury, and R. Parthasarthy, *Physica B* **241**, 403 (1998); R. Mittal, S.L. Chaplot, R. Parthasarthy, M.J. Bull, and M.J. Harris, *Phys. Rev. B* **62**, 12089 (2000).
- ¹⁶A. P. Hammersley, Report No. EXP/AH/95-01, 1995.
- ¹⁷G.-M. Rignanese and X. Gonze, *Phys. Rev. B* **63**, 104305 (2001).
- ¹⁸P. Bruesch, *Phonons: Theory and Experiments* (Springer, Berlin, 1982), Vol. 1.
- ¹⁹S. L. Chaplot (unpublished).
- ²⁰V.K. Jindal and J. Kalus, *Phys. Status Solidi B* **133**, 89 (1986).
- ²¹R. Bhandari and V.K. Jindal, *J. Phys.: Condens. Matter* **3**, 899 (1991).
- ²²R.A. Young, A. Sakthivel, T.S. Moss, and C.O. Paiva-Santos, *J. Appl. Crystallogr.* **28**, 366 (1995).